

Atomic time-of-arrival measurements with a laser of finite beam width

J. A. Damborenea*†, I. L. Egusquiza*, G. C. Hegerfeldt‡ and J. G. Muga†

* Fisika Teorikoaren Saila, Euskal Herriko Unibertsitatea, 644 P.K., 48080 Bilbao, Spain

†Departamento de Química-Física, Universidad del País Vasco, Apdo. 644, 48080 Bilbao, Spain

‡Institut für Theoretische Physik, Universität Göttingen, Bunsenstr. 9, 37073 Göttingen, Germany

Abstract. A natural approach to measure the time of arrival of an atom at a spatial region is to illuminate this region with a laser and detect the first fluorescence photons produced by the excitation of the atom and subsequent decay. We investigate the actual physical content of such a measurement in terms of atomic dynamical variables, taking into account the finite width of the laser beam. Different operation regimes are identified, in particular the ones in which the quantum current density may be obtained.

PACS numbers: 03.65.-w, 42.50-p, 32.80-t

1. Introduction

In spite of the emphasis on “observables” and “measurements” in the standard formulation of quantum mechanics, one of the fundamental difficulties of the theory is to establish the relation between “observables” represented by operators that act on the variables of the microscopic system in isolation, and actual measurements. There is no universal prescription to construct an apparatus for a given operator and, in the other direction, identifying from the macroscopic experiment the corresponding microscopic operator may also be difficult. These problems have been particularly acute, or have been perceived to be so, for time observables. According to an argument due to Pauli [1], there is no self-adjoint time operator conjugate to a semibounded Hamiltonian (see however [2]), and this limitation has hindered the research on the theoretical understanding and description of time quantities measured in the laboratories. The trend is slowly changing though [3]. During the last two decades, many works have been devoted to find consistent theories, in terms of operators or otherwise, about characteristic times for tunneling, quantum jumps, decay, or arrival [4, 3]. This effort has been mostly focused on establishing fundamental theories for the isolated system, typically a structureless particle. In these theories the measuring apparatus is totally absent, at least in an explicit form, or at best modelled very schematically [5, 6]. We have advocated the need for an analysis of more realistic models [4, 7], not only to determine how and if the ideally defined quantities can be measured but also to ascertain what usual operational methods are “really” measuring in the language of system variables. In a previous article [7] we have modelled the measurement by fluorescence of the time of arrival (TOA) of an atom at a given location. An important finding was that, in the limit of *weak driving*, the quantum current density J may be obtained from the distribution of first photon detections Π . This is satisfactory because, in the classical limit, J is the correct TOA distribution for the initial states considered (with momenta fully directed towards the laser); but it is also surprising because J may be negative in quantum mechanics, even for states formed entirely by positive momentum components [8]. By contrast, the positive and axiomatic TOA distribution of Kijowski [9] was not obtained in any limit of the parameters involved, except when it is sufficiently close to J . A simplifying assumption of the model was that the laser-illuminated region had a semi-infinite width, from $x = 0$ to ∞ . This is a good approximation at very low kinetic energies, because the atom is either detected before abandoning the finite illuminated region, or reflected by the laser; but it fails otherwise. In this paper we remove that assumption and consider the more realistic case of a finite laser beam width, L .

There were two basic difficulties with a direct “good TOA measurement” in the semi-infinite model: the atomic reflection with no photon emission, due to a strong laser field, and the detection delay for a weak one. Although we could find and characterize operation regimes where the two effects were negligible in practice, the best fit with the free-motion current density was obtained for weak driving and for a short lifetime $1/\gamma$ of the excited state (γ is Einstein’s coefficient); this avoids reflection but induces

delay because, in spite of the short life time, the laser pumping is very inefficient. Nevertheless, the flux J for the freely moving atoms may be obtained in principle from the experimental signal Π , since, in that limit, $\Pi = J * W$, where W is the (known) distribution of photon detection times corresponding to a laser-illuminated atom at rest.

The applicability of the above “deconvolution” method is limited because the long detection delays implied require also a large laser-beam width, and the required width increases with the atomic velocity. In practice the laser beam is of course always finite, so there is a third problem aside from reflection and delay: atomic transmission through the laser without photon detection, which mainly affects the fast components and may also cause distortion in the measured photon distribution. We shall characterize this effect, and describe several operation regimes. Finally, we shall see how, taking advantage of the Rabi oscillation induced by the laser, the flux may also be obtained by deconvolution with a finite width laser at least in two cases: for *strong driving* and $\gamma \rightarrow 0$, i.e., in a limit which is quite the opposite from the one used for the semi-infinite laser, and when the momentum width of the atomic wave packet is small compared to its average momentum.

2. The model

The setting of the modelled experiment and the fundamental theory are described in Ref. [7] so we shall only outline the basic ideas and equations here, emphasizing the novelties due to the finite laser-beam width. A two-level atom wave packet impinges on a perpendicular laser beam at resonance with the atomic transition. In the so called quantum jump approach [10] the continuous measurement of the fluorescence photons is simulated by a periodic projection onto no-photon or one-photon subspaces every δt , a time interval large enough to avoid the Zeno effect, but smaller than any other characteristic time. The amplitude for the undetected atoms in the interaction picture for the internal Hamiltonian obeys, in a time scale coarser than δt , and using the rotating wave and dipole approximations, an effective Schrödinger equation governed by the complex “conditional” Hamiltonian (the hat is used to distinguish momentum and position operators from the corresponding c-numbers)

$$H_c = \hat{p}^2/2m + \frac{\hbar}{2} \begin{pmatrix} 0 & 0 \\ 0 & -i\gamma \end{pmatrix} + \frac{\hbar}{2} \chi(\hat{x}) \begin{pmatrix} 0 & \Omega \\ \Omega & 0 \end{pmatrix}, \quad (1)$$

where the ground state $|1\rangle$ is in vector-component notation $\begin{pmatrix} 1 \\ 0 \end{pmatrix}$, the excited state $|2\rangle$ is $\begin{pmatrix} 0 \\ 1 \end{pmatrix}$,

$$\chi(x) = \begin{cases} 1, & 0 < x < L \\ 0, & \text{otherwise} \end{cases} \quad (2)$$

and Ω is the Rabi frequency. The probability, N_t , of no photon detection from t_0 , the instant when the packet is prepared far from the laser and with positive momenta, up to time t , is given by [10]

$$N_t = ||e^{-iH_c(t-t_0)/\hbar} |\psi(t_0)\rangle||^2, \quad (3)$$

and the probability density, $\Pi(t)$, for the first photon detection by

$$\Pi(t) = -\frac{dN_t}{dt} = \gamma P_2, \quad (4)$$

where P_2 is the population of the excited state. Π plays the role of an “operational” time-of-arrival distribution. To obtain the time development under H_c of a wave packet incident from the left we first solve the stationary equation

$$H_c \Phi = E \Phi, \quad \text{where } \Phi(x) \equiv \begin{pmatrix} \phi^{(1)}(x) \\ \phi^{(2)}(x) \end{pmatrix} \quad (5)$$

for scattering states with real energy $E = \hbar^2 k^2 / 2m \equiv E_k$, which are incident from the left ($k > 0$),

$$\Phi_k(x) = \frac{1}{\sqrt{2\pi}} \begin{cases} \begin{pmatrix} e^{ikx} + R_1 e^{-ikx} \\ R_2 e^{-iqx} \end{pmatrix}, & x \leq 0, \\ \begin{pmatrix} T_1 e^{ikx} \\ T_2 e^{iqx} \end{pmatrix}, & x \geq L. \end{cases} \quad (6)$$

These states are not orthogonal, in spite of the reality of E , because the Hamiltonian H_c is not Hermitian. The wavenumber q obeys

$$E + i\hbar\gamma/2 = \hbar^2 q^2 / 2m, \quad (7)$$

with $\text{Im } q > 0$ for boundedness, while $R_{1,2}$ and $T_{1,2}$ are reflection and transmission amplitudes yet to be determined for the ground and excited state channels.

To obtain the form of $\Phi_k(x)$ for $0 < x < L$ we denote by $|\lambda_+\rangle$ and $|\lambda_-\rangle$ the (unnormalized and nonorthogonal) eigenstates of the matrix $\frac{1}{2} \begin{pmatrix} 0 & \Omega \\ \Omega & -i\gamma \end{pmatrix}$ corresponding to the eigenvalues λ_\pm ,

$$\lambda_\pm = -\frac{i}{4}\gamma \pm \frac{i}{4}\sqrt{\gamma^2 - 4\Omega^2} \quad (8)$$

$$|\lambda_\pm\rangle = \begin{pmatrix} 1 \\ 2\lambda_\pm/\Omega \end{pmatrix}. \quad (9)$$

(Formally we assume that $\lambda_+ \neq \lambda_-$. The case $\lambda_+ = \lambda_-$ may be treated by taking the limit.) For $0 < x < L$, one can write Φ_k as a superposition of $|\lambda_\pm\rangle$ in the form

$$\sqrt{2\pi}\Phi_k(x) = C_{++}|\lambda_+\rangle e^{ik+x} + C_{-+}|\lambda_-\rangle e^{ik-x} \quad (10)$$

$$+ C_{+-}|\lambda_+\rangle e^{-ik+x} + C_{--}|\lambda_-\rangle e^{-ik-x}, \quad 0 < x < L, \quad (11)$$

which, at variance with the semi-infinite laser case must contain now growing exponentials in addition to decaying ones. From the eigenvalue equation $H_c \Phi_k = E_k \Phi_k$, together with $E_k = \hbar^2 k^2 / 2m$, there follows

$$k_\pm^2 = k^2 - 2m\lambda_\pm/\hbar = k^2 + i\gamma m/2\hbar \mp i\sqrt{\gamma^2 - 4\Omega^2}m/2\hbar, \quad (12)$$

with $\text{Im } k_\pm > 0$. The continuity of $\Phi_k(x)$ and its derivative at $x = 0$ and $x = L$ leads to eight equations with eight unknowns and to explicit but rather lengthy expressions for the coefficients of the wave function in the laser region, see (10), and for the transmission and reflection amplitudes. We shall not display them here but discuss different limits, approximations and numerical examples.

An important simplification occurs for kinetic energies above $\Omega\hbar/2$ or, equivalently, for de Broglie wavelengths $2\pi/k$ smaller than the Rabi-wavelength $2\pi v/\Omega$: the stationary wave may be very well approximated according to the classical idea that the atom moves along an unperturbed classical trajectory, without reflection, and with its internal level populations oscillating quantally in the laser-illuminated region. Specifically, $\Phi(\mathbf{x})$ in the laser region ($0 < x < L$) can be approximated as the product of the internal wave function for the atom at rest, assuming a pure ground state at an entrance instant $t = 0$, and making the substitution $t = x/v$, times the translational plane wave $e^{ikx}/(2\pi)^{1/2}$,

$$\Phi(x) = \frac{e^{ikx} e^{-\gamma x/4v}}{(2\pi)^{1/2}} \begin{cases} \cos[\frac{x}{2v}\sqrt{\Omega^2 - \gamma^2/4}] + \frac{\gamma}{2\sqrt{\Omega^2 - \gamma^2/4}} \sin[\frac{x}{2v}\sqrt{\Omega^2 - \gamma^2/4}] \\ \frac{-i\Omega}{\sqrt{\Omega^2 - \gamma^2/4}} \sin[\frac{x}{2v}\sqrt{\Omega^2 - \gamma^2/4}] \end{cases} \quad (13)$$

whereas to the left of the laser $R_1 \approx R_2 \approx 0$, and to the right the transmission amplitudes $T_{1,2}$ are obtained by continuity from (6) and (13). In particular,

$$T_2 = e^{i(k-q)L} e^{-\gamma L/4v} \frac{-i\Omega}{(\Omega^2 - \gamma^2/4)^{1/2}} \sin\left[\frac{L}{2v}(\Omega^2 - \gamma^2/4)^{1/2}\right]. \quad (14)$$

The validity of this semiclassical approximation for the translational part of the stationary waves does not mean that every wave packet with energy components well above $\Omega\hbar$ behaves classically. Two or more different stationary components may add up coherently in the time dependent wavefunction, leading to very non-classical interference effects, as we shall see in an example below.

If $\tilde{\psi}(k)$ denotes the wavenumber amplitude that the wave packet would have as a freely moving packet at $t = 0$, then

$$\Psi(x, t) = \int_0^\infty dk \tilde{\psi}(k) \Phi_k(x) e^{-i\hbar k^2 t/2m} \quad (15)$$

describes the ‘‘conditional’’ time development of the state for an undetected atom which in the remote past comes in from the left in the ground state.

3. Operation regimes

Figure 1 shows the total detection probability, or ‘‘absorption’’ due to the non-hermitian potential, $A = 1 - |T_1|^2 - |R_1|^2$, versus the incident velocity v and Rabi frequency Ω for the stationary wavevectors Φ_k . A may also be understood as the probability that the particle be reflected or transmitted in state $|2\rangle$, or be detected through a photon emission in the laser region. We may distinguish several regions in the v - Ω plane (these regions are also portraided in figure 2) depending on three basic criteria, each associated with a dimensionless parameter:

- Reflection: Except for very weak driving, where it is not significant, reflection is important for kinetic energies below or around $E = \Omega\hbar/2$, (dashed line in figure 2), but vanishes when $E \gg \Omega\hbar/2$.
- Laser intensity: Strong driving for $\Omega/\gamma > 1$, and weak driving for $\Omega/\gamma < 1$.

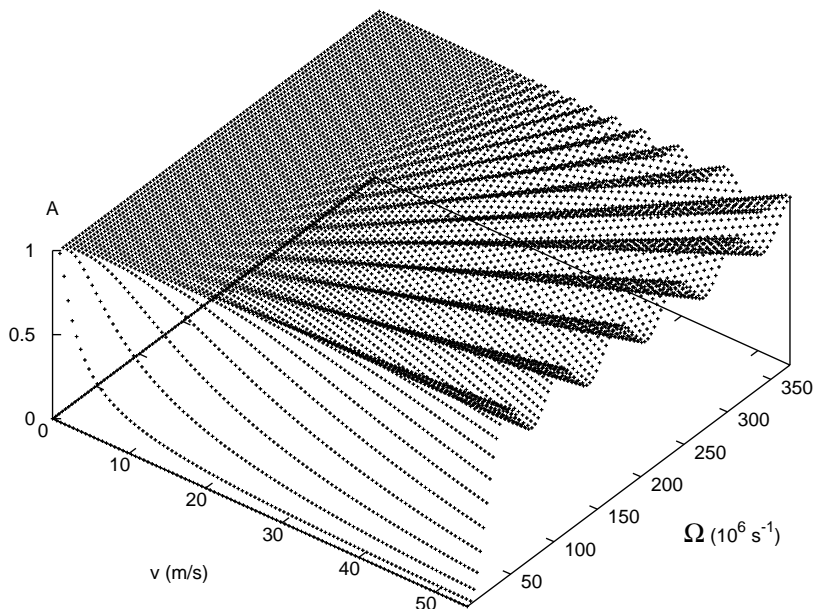


Figure 1. Absorption versus velocity v and Rabi frequency Ω for $L = 5\mu\text{m}$. This and other figures are obtained for the transition at 852 nm of Cs atoms, with $\gamma = 33.3 \times 10^6 \text{ s}^{-1}$.

- Laser beam width: Let l be the “penetration length” of the stationary wave in the semi-infinite laser region, that we may estimate as five times the detection delay [7] multiplied by the atomic velocity v ,

$$l = 5v \left(\frac{2}{\gamma} + \frac{\gamma}{\Omega^2} \right). \quad (16)$$

For $L > l$ the laser behaves effectively as a semi-infinite one. This regime, to the left of the curved solid line of figure 2, corresponds essentially to the one examined in the previous paper. The exact expressions for wave functions, reflection and transmission amplitudes obtained in [7] are good approximations for the finite width laser if $L > l$ but fail otherwise. Figure 3 shows the critical “temperature” versus L (for Cs atoms and $\gamma = 33.3 \times 10^6 \text{ s}^{-1}$) above which the finite width of the laser has to be taken into account.

For a constant Ω , at moderate to strong driving, A increases very sharply from zero to one at low v . This increase is not visible in figure 1 because of the scale, but can be seen in the close-up of figure 4. The small absorption near $v = 0$ is due to reflection into the ground state. After the rapid increase of A at low v along a constant Ω line, there follows a *plateau* of perfect detection, still within the “semi-infinite laser” regime, see again figure 1. Gradually, for higher and higher velocity v and in strong driving conditions, the plateau is substituted by an oscillating pattern. The absorption surface to the right of the plateau resembles a fan, which can be explained in terms of the semiclassical picture and the finiteness of the laser “barrier”. The ridges

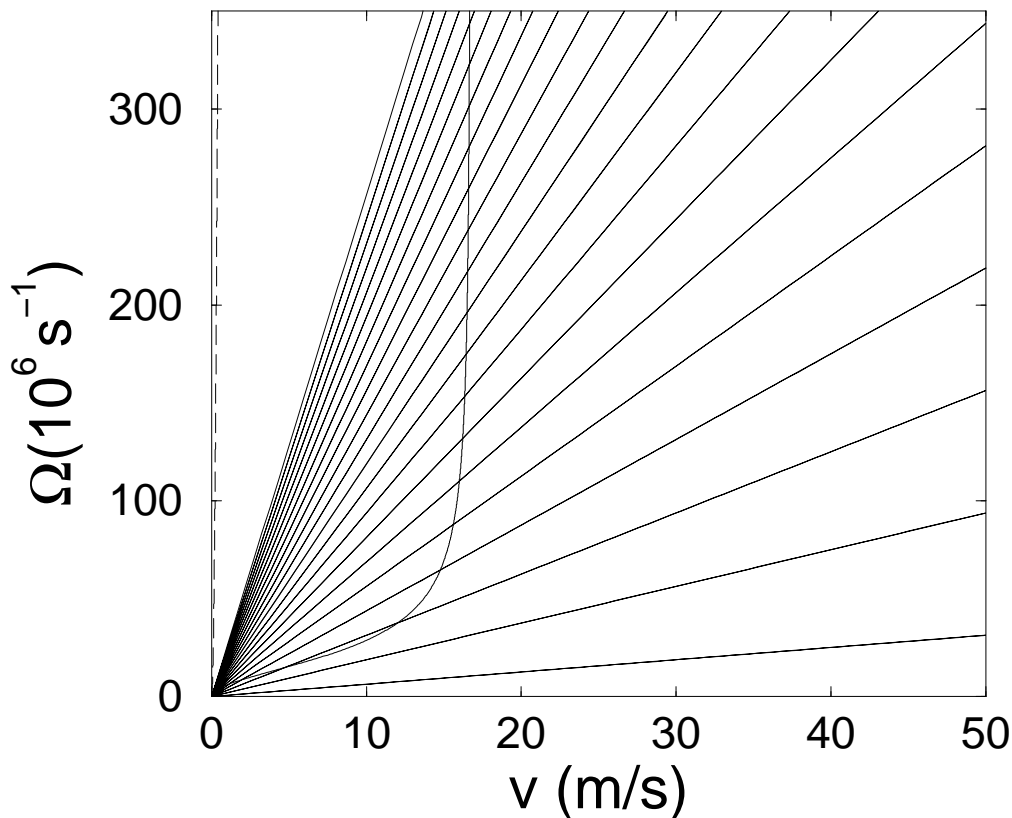


Figure 2. Ω - v plane with separations of the different regions, $L/l = 1$ (curved solid line), $2E/\hbar\Omega = 1$ (dashed line), and maximum absorption lines up to $n = 20$ (straight solid lines), see (18). $L = 5\mu\text{m}$ as in figure 1.

correspond to combinations of parameters where the Rabi oscillation leaves the excited state population at a maximum on the laser edge L , so that the decay takes place behind the laser, at $x > L$, with a detection delay $1/\gamma$ from the instant when the classical trajectory leaves the laser.

Each ridge corresponds to a number $n + 1/2$ of Rabi oscillations between $x = 0$ and $x = L$, and will be indexed by $n = 0, 1, 2, \dots$. Neglecting the effect of γ within the laser region, the velocity at the ridge for a given Ω is given by

$$v_n = \frac{L\Omega}{(2n + 1)\pi}. \quad (17)$$

Equivalently, each absorption ridge may be characterized by the straight line

$$\Omega_n = \frac{(2n + 1)\pi v}{L} \quad (18)$$

in the Ω - v plane. The first one, for $n = 0$, corresponds to a spatial version of a π pulse, i.e., the velocity, laser-beam width, and Rabi frequency are just the right ones to pump the (semiclassical) atom, from the ground state at $x = 0$ to the excited state at $x = L$, in half Rabi oscillation. Note from (17) that the fan structure “folds upwards” by decreasing L , because smaller lengths require higher laser intensities to achieve full

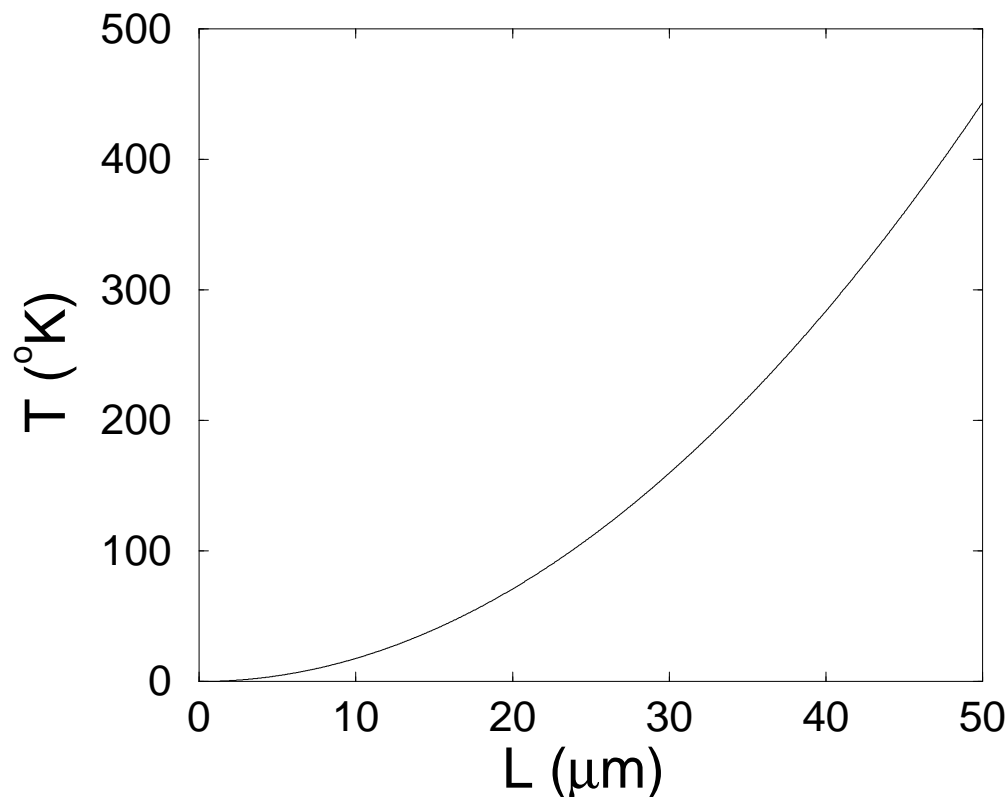


Figure 3. “Critical Temperature”, calculated as mv_L^2/K , versus laser-beam width L for Cesium atoms and strong driving conditions. $v_L = L\gamma/10$, i.e., the velocity for which the penetration length is equal to the laser beam width, $l = L$. $\gamma = 33.3 \times 10^6 \text{ s}^{-1}$, and K is Boltzmann’s constant. Above this temperature the effect of the finite width of the laser beam cannot be ignored.

detection. The minima at the valleys correspond to an entire number of Rabi oscillations. These minima are not exactly zero due to the absorption that takes place in the laser region. As the velocity v increases, however, this absorption decreases, as may be seen in figure 5. Finally, for velocities greater than v_0 , the atom is too fast for being completely excited during the crossing of the laser-illuminated region, and the absorption decreases monotonously. The solid line in figure 5 shows a cut of the absorption surface along a constant- Ω line for strong driving conditions.

The velocity window for nearly complete detection on a ridge along a constant- Ω line is larger for smaller n . This is also clearly illustrated in figure 5. A simple formula for the window width Δ_W around the maximum where absorption is better than 99% is

$$\Delta_W < \left[\frac{2}{\pi(2n+1)} \right]^2 \frac{L\Omega}{10} = \frac{4v_n}{10\pi(2n+1)}. \quad (19)$$

Notice that even in the best case, $n = 0$, a wave packet located essentially within one of these windows of full detection will have a small width Δv compared to its average

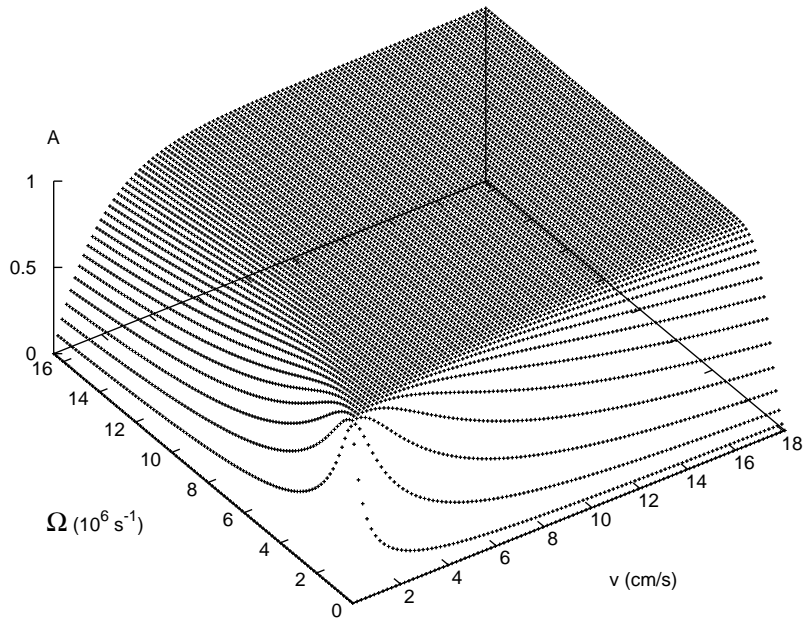


Figure 4. Close-up of figure 1.

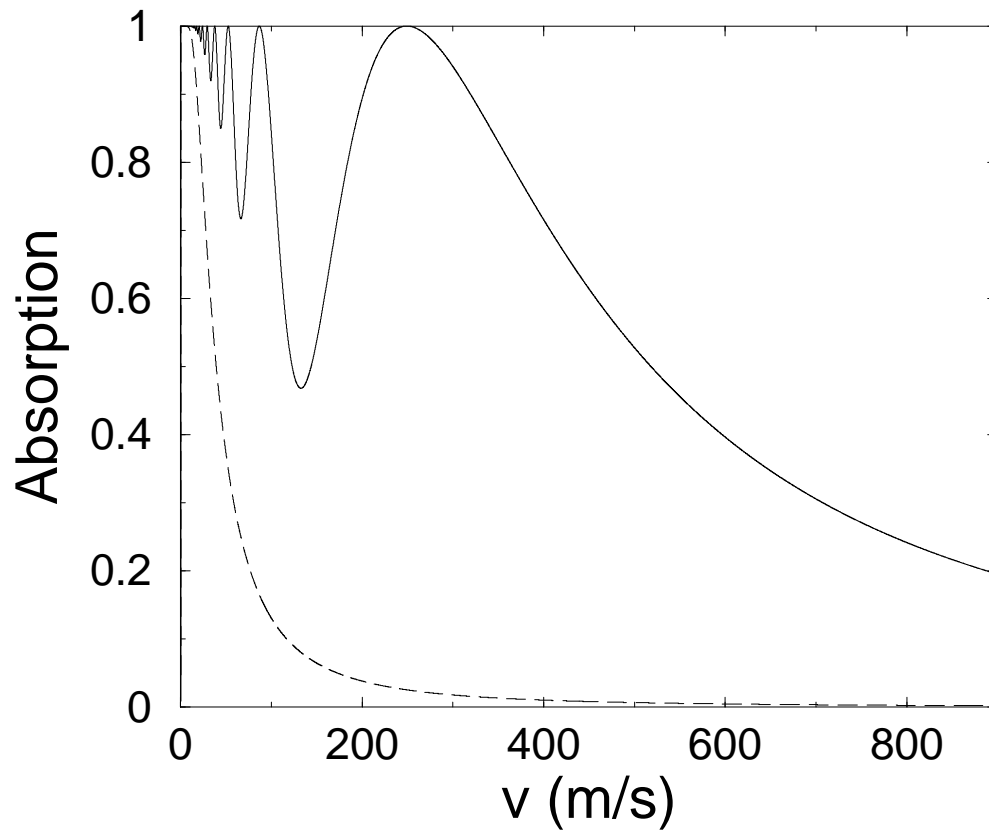


Figure 5. Absorption versus v for $\Omega = 5\gamma$ (solid line), and $\Omega = \gamma/2$. $L = 5\mu\text{m}$.

velocity. In particular, for $\Delta_W = 8\Delta v$,

$$\Delta v \approx \frac{v_n}{(2n+1)60}. \quad (20)$$

An interesting feature of the transmission amplitude T_2 at the detection maxima is its alternating sign, $-i$ for n even, and i for n odd, see (14). We shall comment on physical consequence below.

The above description is not applicable to weak driving conditions. Reflection in particular is less important at low velocities than for strong driving, and it vanishes for any $v \neq 0$ when $\gamma/\Omega \rightarrow \infty$. Also, the plateau of full detection is much narrower than for strong driving, and for higher velocity v along a constant- Ω line, the laser does not have enough intensity to produce Rabi oscillations, so the absorption decays monotonously with v , see figures 1, 4, and 5.

The detection delay for a given incident wavenumber will in general have contributions from the laser region and from the region outside. The delays in the laser region are $2/\gamma$ for strong driving or γ/Ω^2 for weak driving when $L > l$ [7], or fractions of these quantities for smaller laser-beam widths, whereas the detection delay once the (semiclassical) excited atom arrives at L is $1/\gamma$. This later contribution would be very small for large (ideally infinite) γ , but in this limit, with all other parameters constant, there would not be excitation at all. One might then imagine the case where both γ and Ω are infinite, but with a constant ratio Ω/γ . In this case, however, the penetration length goes to zero, and the semi-infinite laser result, $R_1 \rightarrow -1$, applies, so that all atoms would be reflected without being excited [7]. Another not very helpful limit is $L \rightarrow 0$, with all other parameters fixed, because all atoms are transmitted in the ground state without being detected‡. “Good” direct (no delay, full detection) measurements are possible, but only within specific parameter ranges. For moderate velocities, i.e., provided $L > l$ for the wave packet momentum components, and above the reflection region, the measurement on the full-detection plateau can be very efficient, as illustrated in Ref. [7]. This requires, for strong or weak driving,

$$\frac{\hbar}{E} \ll \frac{1}{\Omega} + \frac{\gamma}{\Omega^2} \ll \frac{2}{\gamma} \ll \frac{L}{5v}, \Delta t, \quad (21)$$

where Δt is the time span of the wave packet passage. Even when these conditions are fulfilled, the observed Π is only approximately equal to J . Unfortunately, the deconvolution used in Ref. [7] to get the flux J exactly for large γ may be impossible to implement with a finite-width laser at large velocities, since the penetration length $l \rightarrow \infty$ as $\gamma \rightarrow \infty$. The following section provides a way out which, again, is not universal but depends in fact on rather restrictive conditions.

‡ One might of course insist on using the information of the very few detected atoms and normalize, but the result is strongly biased in favour of the slowest energy components.

4. An ideal distribution

Full detection is achieved sufficiently close to the ridges of the fan structure for moderate to strong driving. The first maximum, corresponding to $n = 0$, is particularly suitable because it provides the largest momentum window of nearly complete absorption. Let us assume that Ω and L may be adjusted so that most of a wave packet lies within an absorption maximum. As in the weak driving case of the semi-infinite laser, full detection comes with a price: the detection delay due to the time necessary to de-excite the atom, now outside the laser illuminated region. We have pointed out already that a short lifetime (a large γ) “solves” this problem but also creates a new one: the absence of excitation and therefore of detection. This suggests that the useful limit may be quite the opposite, namely, $\gamma \rightarrow 0$. The long delay can then be subtracted using a convolution formula to obtain an “ideal” distribution that coincides with the flux when $\gamma \rightarrow 0$, or, quite independently of γ , for narrow wave packets in momentum space.

To define from the “experimental” $\Pi(t)$ an idealized arrival-time distribution, we shall assume

$$\frac{\hbar}{E} \ll \frac{1}{\Omega} \lesssim \frac{L}{v} \ll \frac{1}{\gamma}, \quad (22)$$

so that we can use the semiclassical and strong driving approximations neglecting the effect of γ between 0 and L , since the only significant absorption (i.e., detection) occurs for $x > L$.

$\Pi_{\text{id}}(t)$ is then defined by the convolution formula

$$\Pi = \Pi_{\text{id}} * W, \quad (23)$$

where

$$W(t) = \gamma e^{-\gamma t} \quad (24)$$

is the probability density to detect a photon at time t if the atom is excited at $t = 0$ in the laser-free region. Even though (23) is in fact the equation that *defines* Π_{id} , there is of course a “classical” physical motivation for the convolution structure. If the arrival time of the atom, and the time of photon emission from the arrival instant were independent random variables, then the distribution for the sum of these two quantities would have precisely that form. It turns out, as discussed in Ref. [7] that Π_{id} may become negative so, generically, this simple hypothesis does not hold true quantum mechanically. This does not invalidate Π_{id} , but should make us cautious about its interpretation: it *plays the role* of a time of arrival density in quantum mechanics, but does not share all the properties of the corresponding classical density, most prominently positivity. This resembles the status of the Wigner function, which plays the role of a classical phase-space probability density but can also be negative.

The ideal distribution Π_{id} is obtained from the relation between Fourier transforms, $\tilde{\Pi}_{\text{id}} = \tilde{\Pi}/\tilde{W}$ where $\tilde{\Pi}(\nu) = \int dt e^{-i\nu t} \Pi(t)$ etc. From (24) one finds

$$\tilde{W}(\nu) = \frac{\gamma}{i\nu + \gamma}, \quad (25)$$

so that, in the time domain,

$$\Pi_{\text{id}}(t) = \Pi(t) + \frac{1}{\gamma}\Pi'(t). \quad (26)$$

If the wave packet is centered at one of the absorption maxima, and the momentum width satisfies (19), the atoms are all pumped to the excited state, $|T_2| \approx 1$, and we may write

$$\Pi(t) = \frac{\gamma}{2\pi} \int_L^\infty dx \int dk \int dk' \tilde{\psi}(k) \tilde{\psi}^*(k') e^{-i(E-E')t/\hbar} e^{i(q-q^*)x}. \quad (27)$$

Performing the x integral, and approximating the resulting denominator according to (22),

$$q - q^* \approx k - k' + \frac{i\gamma m}{2\hbar} \frac{k + k'}{kk'}, \quad (28)$$

one finally gets

$$\begin{aligned} \Pi_{\text{id}}(t) &= \frac{1}{2\pi} \int \int dk dk' e^{-i(E-E')t/\hbar} e^{i(k-k')L} \tilde{\psi}(k) \tilde{\psi}^*(k') \\ &\quad \times \left[\frac{i\gamma + (k^2 - k'^2)\hbar/2m}{(k - k') + \frac{i\gamma m}{2\hbar} \left(\frac{k+k'}{kk'} \right)} \right]. \end{aligned} \quad (29)$$

The term in square brackets tends to the kernel of the integral that gives the current density J ,

$$\frac{(k + k')\hbar}{2m}, \quad (30)$$

in several limits. Using $k' = k + \delta$, this occurs in particular for $\gamma \rightarrow 0$, and also for $\delta/k \rightarrow 0$ independently of the value of γ , as long as (22) is satisfied. In this later case, namely for a small momentum width in comparison to the momentum itself, (30) coincides also with the kernel of Kijowski's axiomatic TOA distribution,

$$\frac{(kk')^{1/2}\hbar}{m}, \quad (31)$$

since $k \approx k'$ and the arithmetic and geometric means in (30) and (31) coincide. The condition of small momentum-width also implies that the effect of the derivative in (26) is negligible, and that, even if the last inequality of (22) fails, J can be obtained very accurately by normalizing the observed results. An example is shown in figure 6, where two Gaussians on the top of a single ridge have been added coherently,

$$\psi = \psi_a + \psi_b, \quad (32)$$

to produce an interference pattern in the flux.

According to (20), the condition $\Delta v/\langle v \rangle \ll 1$ is necessarily fulfilled when the wave packet momenta are within one ridge of maximum detection, so that the flux and Kijowski's distribution will coincide, i.e., no negative values of J may be found in this case. In order to measure backflow the wave packet must be located within the full detection plateau and then proceed as in Ref. [7] but the finite width of the laser beam imposes a maximum speed for this method to work. Another route would be to use

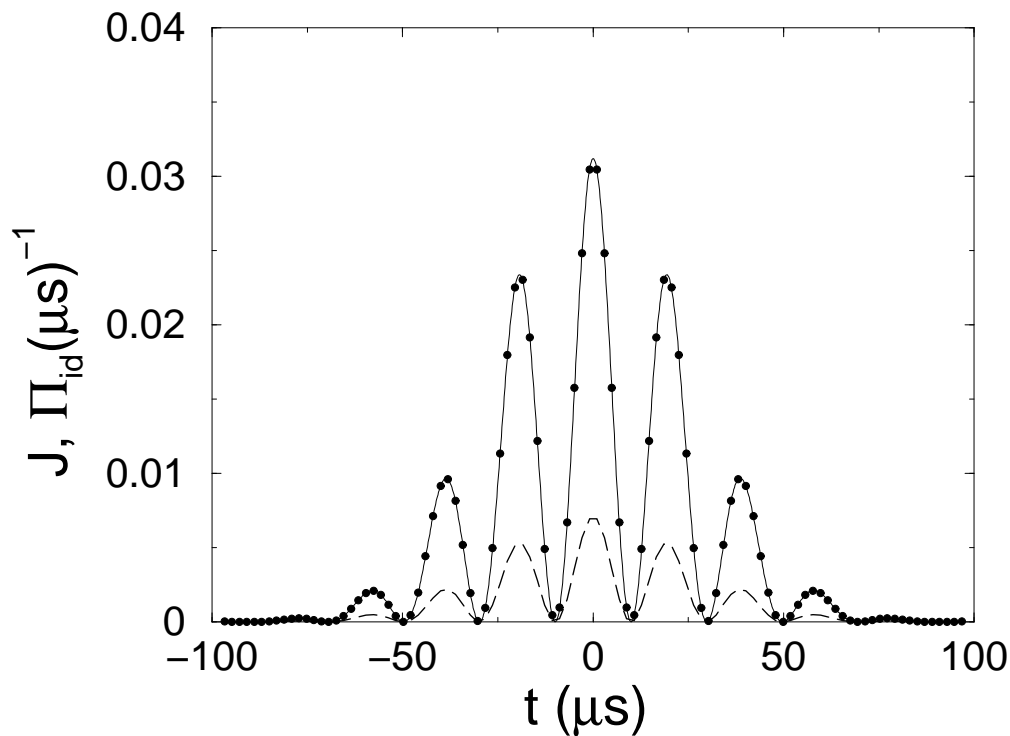


Figure 6. Flux (solid line), Π_{id} (dashed line), and normalized Π_{id} (dots), for the coherent sum of two Gaussians with average velocities $v_1 = 167.05\text{m/s}$ and $v_2 = v_1 + .9\mu\text{m/s}$, and $\Delta x = 4233\mu\text{m}$. They become minimal-uncertainty-product states when their centers arrive at $L = 5\mu\text{m}$. $\Omega = 104.43 \times 10^6 \text{ s}^{-1}$.

different ridges of maximum detection for each gaussian. The two gaussians should be on odd or even n ridges but not on contiguous ones because of the sign change of the transmission amplitude mentioned below (20).

5. Conclusions

In this paper we have analyzed the measurement of the arrival time of an atom at a given location by means of a laser that illuminates a finite region. Repeating the experiment many times for a given atomic preparation produces an “observed distribution” of first fluorescence photons Π , that will in general be distorted with respect to the “axiomatic” distribution of Kijowski Π_K or the flux J (both evaluated for the isolated atom, i.e., without the laser) because of detection delay, and atomic reflection or transmission without photon detection. (In general even if the three problems are made negligible Π is only approximately equal to these “ideal” quantities.) It is possible to correct for the distortions due to detection delays, at least in certain limits, and obtain the current density by deconvolution. In the present model the laser beam intensity has sharp edges to facilitate the analytical examination but very similar results have been obtained for a more realistic Gaussian profile, see figure 7.

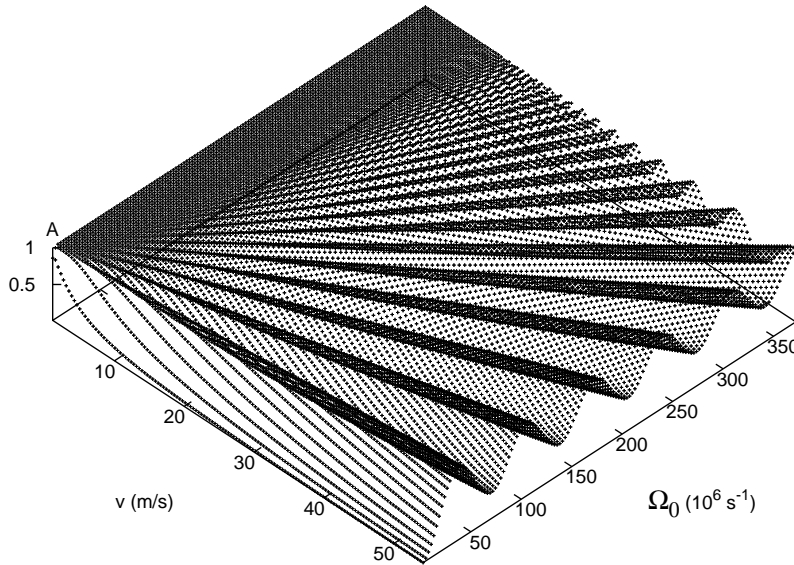


Figure 7. Absorption versus velocity v and Ω_0 for $L = 5\mu\text{m}$ and position dependent Rabi frequency, $\Omega(x) = L\Omega_0 e^{-\frac{(x-x_0)^2}{2\delta^2}} / \delta(2\pi)^{1/2}$; $\delta = 0.529\mu\text{m}$, $x_0 = 2.5\mu\text{m}$, and $\gamma = 33.3 \times 10^6 \text{ s}^{-1}$. The calculation is performed with a transfer matrix method.

Acknowledgments

This work has been supported by Ministerio de Ciencia y Tecnología (BFM2000-0816-C03-03), UPV-EHU (00039.310-13507/2001), and the Basque Government (PI-1999-28).

References

- [1] Pauli W 1958 in *Handbuch der Physik* (Encyclopedia of physics) (ed. S. Flufge) vol 5 (Berlin: Springer) p 1-168
- [2] Galapon E A 2002 Proc. Roy. Soc. London A **458** 451
- [3] Muga J G, Sala R and Egusquiza I L 2002 (eds) *Time in Quantum Mechanics* (Berlin: Springer)
- [4] Muga J G and Leavens C R 2000 Phys. Rep. **338** 353
- [5] Aharonov Y, Oppenheim J, Popescu S, Reznik B and Unruh W G 1998 Phys. Rev. A **57** 4130
- [6] Halliwell J J 1999 Prog. Theor. Phys. **102** 707
- [7] Damborenea J A, Egusquiza I L, Hegerfeldt G and Muga J G 2002 Phys. Rev. A **66** 052104
- [8] Up to 4% of the norm can go backwards, cf. Bracken A J and Melloy G F 1994 J. Phys. A: Math. Gen. **27** 2197. For this backflow effect see also Allcock G R 1969 Ann. Phys. (N.Y.) **53** 311 and Muga J G, Palao J P and Leavens C R 1999 Phys. Lett. A **253** 21
- [9] Kijowski J 1974 Rep. Math. Phys. **6** 361; Werner R 1986 J. Math Phys. **27** 793; Muga J G, Leavens C R and Palao J P 1998 Phys. Rev. A **58** 4336; Baute A D, Sala Mayato R, Palao J P, Muga J G and Egusquiza I L 2000 Phys. Rev. **61** 022118; Baute A D, Egusquiza I L, Muga J G and Sala Mayato R 2000 Phys. Rev. A **61** 052111; Baute A D, Egusquiza I L, and Muga J G 2001 Phys. Rev. **64** 012501; Baute A D, Egusquiza I L and Muga J G 2001 Phys. Rev. A **64**, 014101; Baute A D, Egusquiza I L, and Muga J G 2002 Phys. Rev. A **65** 032114

- [10] Hegerfeldt G C and Wilser T S 1993 in: *Classical and Quantum Systems* Proceedings of the Second International Wigner Symposium, July 1991, edited by H. D. Doebner, W. Scherer, and F. Schroeck (Singapore: World Scientific, Singapore, 1992) p 104; Hegerfeldt G C 1993 Phys. Rev. A **47** 449; Hegerfeldt G C and Sondermann D G 1996 Quantum Semiclass. Opt. **8** 121. For a review cf. Plenio M B and P. L. Knight 1998 Rev. Mod. Phys. **70** 101. The quantum jump approach is essentially equivalent to the Monte-Carlo wavefunction approach of Dalibard J, Castin Y and Mølmer K 1992 Phys. Rev. Lett. **68** 580, and to the quantum trajectories of Carmichael H 1993 *An Open Systems Approach to Quantum Optics*, Lecture Notes in Physics m18, (Berlin: Springer).